



Oxytocin Receptor Expression in Hair Follicle Stem Cells: A Promising Model for Biological and Therapeutic Discovery in Neuropsychiatric Disorders

Sareh Pandamooz^{1,2} · Mohammad Saied Salehi^{2,3}  · Benjamin Jurek^{2,4} · Carl-Philipp Meining² · Negar Azarpira⁵ · Mehdi Dianatpour¹ · Inga D. Neumann²

Accepted: 27 July 2023

© The Author(s), under exclusive licence to Springer Science+Business Media, LLC, part of Springer Nature 2023

Abstract

The intricate nature of the human brain and the limitations of existing model systems to study molecular and cellular causes of neuropsychiatric disorders represent a major challenge for basic research. The promising progress in patient-derived stem cell technology and in our knowledge on the role of the brain oxytocin (OXT) system in health and disease offer new possibilities in that direction. In this study, the rat hair follicle stem cells (HFSCs) were isolated and expanded in vitro. The expression of oxytocin receptors (OXTR) was evaluated in these cells. The cellular viability was assessed 12 h post stimulation with OXT. The activation of OXTR-coupled intracellular signaling cascades, following OXT treatment was determined. Also, the influence of OXT on neurite outgrowth and cytoskeletal rearrangement were defined. The assessment of OXTR protein expression revealed this receptor is expressed abundantly in HFSCs. As evidenced by the cell viability assay, no adverse or cytotoxic effects were detected following 12 h treatment with different concentrations of OXT. Moreover, OXTR stimulation by OXT resulted in ERK1/2, CREB, and eEF2 activation, neurite length alterations, and cytoskeletal rearrangements that reveal the functionality of this receptor in HFSCs. Here, we introduced the rat HFSCs as an easy-to-obtain stem cell model that express functional OXTR. This cell-based model can contribute to our understanding of the progression and treatment of neuropsychiatric disorders with oxytocinergic system deficiency.

Keywords Hair follicle Stem Cell · Oxytocin Receptor · Oxytocin · Psychopathology · Model System

Introduction

The development of effective strategies to treat neuropsychiatric disorders is a global challenge of the twenty-first century. Despite some progress made in recent decades, the knowledge of underlying molecular and cellular causes of most psychopathologies like autism spectrum disorder (ASD) or generalized anxiety disorder (GAD) remains limited. These mental illnesses are complex and multifactorial in nature, rendering it challenging and almost impossible to create accurate animal models [1]. Thus, developing disease-relevant tissue and cellular model systems could address current bottlenecks in the drug discovery process of these diseases [2]. However, patient brain biopsies and their post-mitotic neurons are inaccessible. The use of stem cell technology has provided a number of promising avenues for novel biological and therapeutic discoveries for neuropsychiatric disorders [3]. The generation of induced pluripotent stem cells (iPSCs) through reprogramming of

✉ Mohammad Saied Salehi
saied_salehi@sums.ac.ir

✉ Inga D. Neumann
inga.neumann@biologie.uni-regensburg.de

¹ Stem Cells Technology Research Center, Shiraz University of Medical Sciences, Shiraz, Iran

² Department of Molecular and Behavioural Neurobiology, University of Regensburg, Regensburg, Germany

³ Clinical Neurology Research Center, Shiraz University of Medical Sciences, Shiraz, Iran

⁴ Research Group Neurobiology of Stress Resilience, Max Planck Institute of Psychiatry, Munich, Germany

⁵ Transplant Research Center, Shiraz University of Medical Sciences, Shiraz, Iran

patient fibroblasts, peripheral blood, keratinocytes, hair follicles, and other somatic cell types offers great potential to overcome the obstructions currently impeding the progress toward a better understanding and optimal treatment of mental disorders [4]. The ability of iPSCs to produce otherwise inaccessible cells, such as neurons, represents their main advantage [5]. Crucially, iPSC models provide a scalable platform to study genotype–phenotype correlations for complex genetic disorders and are suitable for high-throughput screening of therapeutic agents [6]. To date, the iPSC technology has proven largely successful in modeling and recapitulating a variety of neuropsychiatric diseases in vitro [7]. Its combination with CRISPR-Cas9 genome editing technologies makes it a powerful tool to elucidate disease mechanisms [8, 9]. Although iPSC models address several challenges associated with studying mental illness, notable limitations remain. Upon reprogramming of somatic cells, not only the cellular lineage identity is reset, but the epigenetic landscape of the cell is erased as well. This poses a significant challenge to the study of neuropsychiatric disorders, which are largely influenced by epigenetic modifications. Other limitations of iPSCs are the relative high cost of required reagents, and the time-consuming nature of generating iPSCs and their differentiation into neurons [10]. The development of a sister technology, directly converting fibroblasts to functional-induced neurons (iNs) [11], provides a valid alternative to conventional iPSCs. This transdifferentiation strategy circumvents the issue of epigenetic erasure and could be a valid alternative for the modeling of environmentally induced neuropsychiatric diseases [12]. Application of iPSCs and iNs has provided a unique molecular/cellular insight into neuropsychiatric disorders. However, technical variability in the generation of neural cells hinders progress in both strategies. Thus, using a cell type that recapitulates the molecular and cellular signatures of neural cells, is easy to obtain, and has reasonable cultivation and differentiation ability can benefit the field. Since 2013, our research group has been studying the characteristics and regenerative potential of hair follicle-derived stem cells (HFSCs) of rats and human [13–18]. These multipotent stem cells are located in the bulge region of hair follicles throughout adulthood, are ontologically related to the nervous system and show a high level of physiological plasticity [19]. In the current study, we investigated the expression of oxytocin receptor (OXTR) in HFSCs migrated from the bulge region of rat hair follicles. The oxytocin (OXT) system, including the OXTR, play a pivotal role in the regulation of socio-emotional behaviors [20–22]. It has been suggested that dysregulations in the oxytocinergic system, including genetic and epigenetic modifications, alterations in OXT and OXTR expression patterns, and OXTR-mediated intracellular signaling cascades might contribute to various psychopathophysiology [23, 24]. According to numerous

studies, single nucleotide polymorphisms (SNP) in the *Oxtr* are associated with ASD, depression, and schizophrenia [25]. Also, differential DNA methylation of the *Oxtr* as a major epigenetic modification may play an important role in the regulation of social behavior and the development of social anxiety [26, 27]. In patients suffering from schizophrenia, reduced expression of OXTR has been reported in the posterior medial temporal cortex [28]. In autism, reduced OXTR expression was found in the superior temporal gyrus [29], whereas in patients with bipolar disorders and depression enhanced expression of OXTR was documented in the prefrontal cortex [30]. Translational animal models, including prairie voles [31, 32] and multiple mouse models of ASD [33–35] have been developed to expand our knowledge about contributions of the oxytocinergic system to ASD, GAD, and schizophrenia. Despite the availability of animal models that shed light on the role of OXT and OXTR, the number of patient-derived stem cell models linked to this neuropeptide and its receptor remains negligible. In this regard, we assess the expression levels of OXTR in migrated stem cells of hair follicles and evaluate its functionality through responding to OXT stimulation. Hence, we introduce here a novel cellular platform for biological and therapeutic studies of neuropsychiatric disorders associated with oxytocinergic system deficiency. It has been well documented that upon OXTR binding, OXT induces a set of intracellular signaling cascades, of which ERK1/2-CREB is the most prominent one [36–38]. In addition to the activation of CREB and modulation of transcriptional processes, OXT was also described to regulate the translation factor eukaryotic elongation factor 2a (eEF2a) [39], essential for translation and protein synthesis. In turn, synthesized proteins may influence cellular responses, such as structuring of cellular processes termed neurites. Neurite outgrowth or retraction can be modulated by altered cytoskeleton stress fiber formation [40]. Therefore, we focused on activation of downstream signaling pathways, alteration of neurite length and cytoskeletal rearrangement to define the functionality of OXTR in target HFSCs, following OXT stimulation. In this study, we introduce the rat HFSCs as an easy-to-obtain stem cell model that is ontologically connected to the nervous system, which can be used to investigate cellular responses toward OXTR activation. This cell-based model will ultimately contribute to our understanding of the progression and treatment of neuropsychiatric disorders with oxytocinergic system deficiency.

Materials and Methods

In the current study, four 3-week old (male, 30–50 g) and four newborn (post-natal day 1–3) Wistar rats were used for isolation of hair follicle stem cells and astrocyte culture,

respectively. The efforts were made to minimize animal suffering and reduce the number of animals used.

Cell Line and Primary Cultures

H32 cells (rat hypothalamic neuronal cell line) were cultured in DMEM/F12 (Sigma-Aldrich, # N6658) supplemented with 10% fetal bovine serum (FBS, Capricorn Scientific, # FBS-HI-11A) and 1% penicillin/streptomycin (Sigma-Aldrich; # P4333). Primary rat cortical astrocytes were obtained from newborn rats, as previously described [41]. Here, cells were cultured in DMEM/high glucose (Sigma-Aldrich; # D6429) supplemented with 10% FBS, 1% penicillin/streptomycin, 1% non-essential amino acid solution (Sigma-Aldrich, # M7145) and 1% L-Glutamine (Life Technologies; #35,050,038).

To isolate rat hair follicle stem cells, the bulge of hair follicles was micro-dissected from the whisker pad of 3-week old rats, as previously described by our group [13]. Briefly, the hair follicles were dissected and mechanically cleaned to remove dermal and adipose tissues. Next, the dermal papilla and hair follicle capsule were removed and discarded, the bulge region was excised and explanted onto collagen (1 mg/ml, Roche; #11,179,179,001) coated 4-well plates. The culture medium was alpha-modified minimum essential medium (Gibco, Ref: 12,561–056) supplemented with 10% FBS, 10% day 11 chick embryo extract (Life Science Production, #MD-004 UK), 1% penicillin/streptomycin, 1% non-essential amino acid solution, and 1% L-Glutamine. The bulges were incubated in humidified atmosphere at 37°C, 5% CO₂. Following migration from hair bulges, stem cells were

passaged at nearly 80% confluency, using 0.25% Trypsin/EDTA (Sigma, #T4049), and were used according to the respective experiment. To assess the ability of these stem cells to form spheres, the trypsinized stem cells were seeded on 1% agarose coated 96-well plates at a density of 5×10^3 cells in a volume of 200 μ l per well, as previously described [42]. Characterization of migrated stem cells and evaluation of OXTR expression were both carried out after the first subculture routine (P1) and before their treatment (P4, Data not shown) to confirm the identity of stem cells and expression of OXTR. Protein extraction, morphological assessments, and viability/proliferation assays were performed at 10 min, 3 h and 12 h post stimulation of HFSCs (P4) with 100, 500, or 1000 nM OXT (Fig. 1). Accordingly, the following experimental groups were assigned: HFSC treated with (i) 100 nM OXT; (ii) 500 nM OXT; (iii) 1000 nM OXT; and (iv) non-treated stem cells (Control: CTRL).

Immunofluorescent Staining

Cells were seeded in 4-chamber glass slides at a density of 7.5×10^4 cells per chamber. To fix the cells, 4% paraformaldehyde (PFA) was added to the cell culture medium (1:1) for 2 min, afterwards the medium was aspirated and 1 ml 4% PFA added to each well for another 10 min. Following, three washes with PBS-T, cells were blocked with blocking solution (0.1% Triton X-100, 1% FBS, 10% NGS prepared in PBS) for 30 min and incubated in diluted primary antibody solution (0.5% Triton X-100, 3% FBS prepared in PBS) overnight at 4 °C. Primary antibodies were used as follows: mouse anti-neslin monoclonal antibody

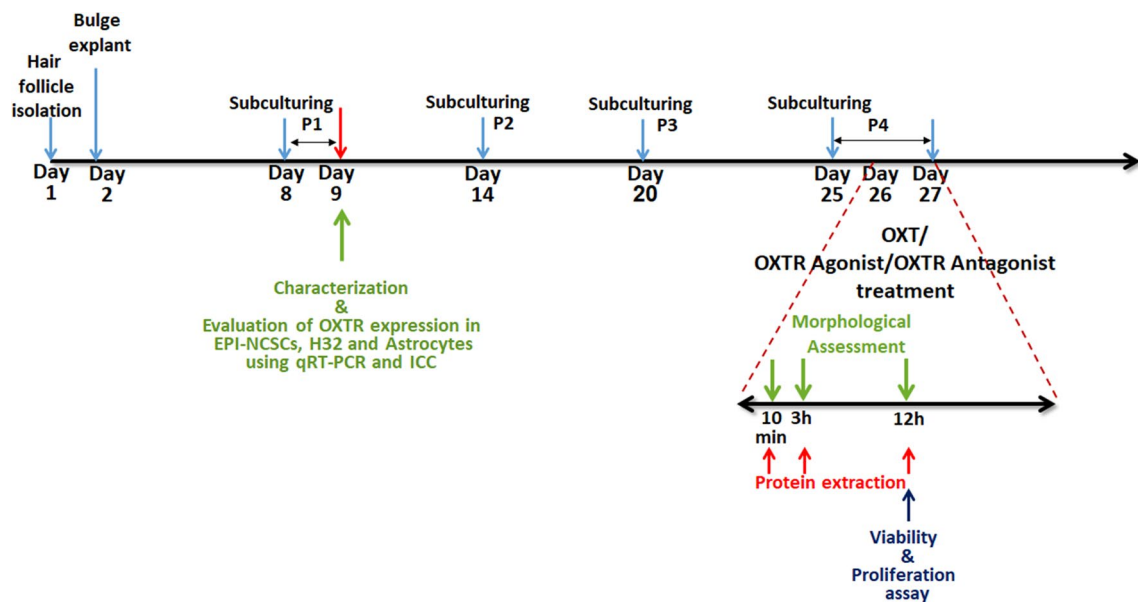


Fig. 1 Schematic time-line protocol of the study

(1:50; Abcam, #ab6142), rabbit anti-SOX10 polyclonal antibody (1:100, Proteintech, #10,422-1-AP), mouse anti-beta III Tubulin monoclonal antibody (1:1000, Abcam, #ab78078), mouse anti-MAP2 monoclonal antibody (1:200, Abcam, #ab11267), rabbit anti-GFAP monoclonal antibody (1:500, Cell Signaling, #12389s), rabbit anti-oxycytocin receptor polyclonal antibody (1:100, Alomone labs, #AVR-013), Phalloidin-AlexaFluor488 (1:200, Cell Signaling, #cs8878) Phalloidin-iFluor594 (1:1000, Abcam, #ab176757). The following day, cells were washed 3 times with PBS-T, re-blocked with 3% BSA for 10 min, and incubated in secondary antibody for 2 h at room temperature (RT). Secondary antibodies were applied as follows: goat anti-rabbit IgG AlexaFluor488 (1:1000, ThermoFisher, #A-11008), goat anti-rabbit IgG AlexaFluor488 (1:1000, Abcam, #ab150085), goat anti-rabbit IgG AlexaFluor594 (1:1000, ThermoFisher, #A11012), goat anti-mouse IgG AlexaFluor488 (1:1000, Abcam, #ab150117), and goat anti-mouse AlexaFluor594 (1:1000, ThermoFisher, #A11032). Finally, the surface of each chamber was covered with one drop of ProLong™ Glass Antifade Mountant with NucBlue™ Stain (Invitrogen, #P36985) that contained DAPI for counterstaining and coverslip used to avoid sample drying. Images were captured with a Leica DM5000B epifluorescence microscope. The immunostaining was performed in triplicate and repeated trice.

RNA Isolation and Quantitative Reverse Transcription-Polymerase Chain Reaction

Total RNA was extracted from hair follicle stem cells grown in 6-well plates at ~90% confluency, using RNeasy mini kit (Qiagen, #74,104) according to the manufacturer's instructions, followed by DNase I (Qiagen, #79,254) treatment and measurement of total RNA concentration and purity using NanoDrop spectrophotometer (Thermo Scientific, Waltham, USA). cDNA was synthesized from 1 µg total RNA using SuperScript® IV Reverse Transcriptase (Invitrogen, #18,090,010). Then, real time-PCR was performed in triplicate using PowerUp™ SYBR® Green Master Mix (ThermoFisher, #A25743) and OXTR primers (listed in Table 1) on a QuantStudio 3 Real Time PCR System (ThermoFisher). According to the MIQE-guidelines [43] we report the following PCR cycle conditions: 50°C for 2min, 95°C for 2min,

followed by 40 cycles of 95°C for 3s and 60°C for 30s. The reference genes *Gapdh* and *Rpl13A* were used as internal reference controls. The $2^{-\Delta\Delta C_t}$ method was used to calculate the relative changes in expression of the target genes.

Cell Viability Assay

Cellular viability was assessed using the PrestoBlue Cell Viability Assay (Invitrogen, #A13261) according to the manufacturer's instruction. Briefly, 2×10^4 cells per well were seeded 12h before the test in a 96-well-plate in 90µl growth- or stimulation medium. Following treatment with different concentrations of OXT, 10 µl of PrestoBlue Reagent was added directly to the cells, incubated for 3 h, before reading the fluorescence intensity with a FluoStar Plate reader (BMG). This experiment was performed in triplicate and repeated trice.

Western Blot

Proteins were extracted from hair follicle stem cells grown in 6-well plates by washing the cells twice with ice-cold PBS, followed by scraping the cells in ice-cold PBS, collecting the cell pellet by centrifugation at 500 g, and immersion in RIPA buffer (Sigma Aldrich, #R0278) with 0.5M EDTA (Thermo Scientific, #1,861,283) and HALT protease and phosphatase inhibitor cocktail (Thermo Scientific, #1,861,284). The whole-cell lysate was kept on ice for 30 min and vortexed vigorously every 10 min. Following 15 min centrifugation at 16,000 g, the protein lysate was collected, and protein concentration was quantified using the BCA protein assay kit (Thermo Fisher Scientific, #23,225). Protein extract separation (20 µg/lane) was performed on a 12% Criterion™ TGX Stain-Free™ Protein Gel (Bio-Rad, #5,678,045). After activating the reaction between the proteins and trihalo compounds in the gel, separated proteins were transferred to a nitrocellulose membrane (Bio-Rad, Trans-Blot Turbo Midi 0.2 µm Nitrocellulose Transfer Packs, #1,704,159) for 30 min at 25 V using the Trans-Blot Turbo System (Bio-Rad; 1,704,150). The membrane was blocked for 1 h in either 5% BSA or 5% milk powder at RT and incubated with the primary antibody overnight at 4°C (Table 2). The next day, membranes were washed trice and incubated with the

Table 1 List of primers and their respective amplicon length in this experiment

Gene	Forward primer (5'-3')	Reverse primer (5'-3')	Amplicon length [bp]
<i>Oxtr</i>	CTGGAGTGTCTCGAGTTGGACC	AGCCAGGAACAGAATGAGGC	136
<i>Gapdh</i>	TGATGACATCAAGAAGGTGG	CATTGTCATACCAGG AAATGAG	185
<i>Rpl13A</i>	ACAAGAAAAAGCGGA TGGTG	TTCCGGTAATGGATC TTTGC	172

Table 2 The list of antibodies used in immunoblotting experiment with their respective concentrations

Primary Antibody	Secondary Antibody
P44/42 MAPK (Erk1/2) Cell Signaling #9102 1:1000 in 5% BSA	Anti-rabbit IgG, HRP-linked Cell Signaling #7074S 1:1000 in TBS-T
Phospho-p44/42 MAPK (pErk1/2) (Thr202/Tyr204) Cell Signaling #9101 1:5000 in 5% BSA	Anti-rabbit IgG, HRP-linked Cell Signaling #7074S 1:1000 in TBS-T
pCREB (Ser133) Millipore #06519 1:5000 in 5% BSA	Anti-rabbit IgG, HRP-linked Cell Signaling #7074S 1:5000 in 5% BSA
peEF2 (Thr56) Cell Signaling #2331 1:1000 in 5% BSA	Anti-rabbit IgG, HRP-linked Cell Signaling #7074S 1:1000 in TBS-T

respective secondary antibody, conjugated to horseradish peroxidase for 1h at RT, followed by three washes for 5 min. To visualize target proteins, the membrane was incubated with Clarity™ Western ECL Substrate (Bio-Rad, # 1,705,062). After 5 min the membrane was exposed and imaged on a Bio-Rad Gel Doc XR Imager system. The resulting images were quantified using Bio-Rad ImageLab 6.0.1 software and stainfree total protein method as loading control. The immunoblotting for each target protein was performed in triplicate and repeated trice.

Morphological Assessment

Neurite Length Measurement

To measure neurite length, cells were seeded on 12-well plate at a density of 1.5×10^5 cells/plate. Cells were treated with OXT (100, 500, 1000 nM; and following 10 min, 3 and 12 h; # 4,016,373, Bachem), or OXTR agonist (TGOT; 100, 500 1000 nM; 12 h; #4,013,837, Bachem) or OXTR antagonist (L-371,257; 1 mM; #2410, Tocris) which was applied 30 min before OXT treatment. Next, cells were gently fixed by adding 1 ml 4% PFA to each well. After 2 min, this solution was discarded and replaced with by 4% PFA for another 10 min. The fixed cells were washed three times with PBS and cells were stained with crysel violet solution (1%, Merck, # 1.15940.0025). The neurite length was determined by manually tracing the length of the longest neurite per cell, from the edge of the nucleus to the apical end of the projection (using the measuring tool in ImageJ Fiji version 1,52r software, NIH, USA). It is worth noting that this experiment was performed in triplicate and repeated trice.

Intensity Measurement

To perform intensity measurements, hair follicle stem cells were seeded in 4-well chamber slide at a density of 4×10^3 cells/chamber. All experimental groups were fixed and blocked as described in the Immunofluorescent staining section. Cells were incubated with AlexaFluor488 Phalloidin (1:200, Cell Signaling, # cs8878) for 10 min to fluorescently stain the cytoskeleton through the binding of phalloidin to F-actin. Finally, slides were mounted with ProLong™ Glass Antifade Mountant with NucBlue™ Stain (Invitrogen, # P36985). The quantitative analysis of fluorescent intensity was performed using ImageJ software (Version 1.52e) on images captured with a Leica DM5000B epifluorescence microscope. The fluorescence intensity was calculated by averaging the fluorescence intensity of all pixels and subtracting the non-specific background from outside the cell. This assessment was conducted in triplicate and repeated trice. It is worth noting that during image acquisition, identical acquisition parameters have been maintained, and saturation of image pixels was controlled by LUT-guided avoidance of blue (saturated) pixels.

Statistical Analysis

The statistical analysis was performed with GraphPad Prism (Version 7.03, GraphPad Software Inc., San Diego, CA) using a one-way analysis of variance (ANOVA) and Tukey post hoc analyses. Separate statistical analyses were conducted using the t-test. Statistical significance was accepted at $p < 0.05$. The data are presented as mean \pm SEM.

Results

Characterization of Hair Follicle Stem Cells

Few days after bulge explantation, migrated stem cells with stellate morphology were observed around the bulges (Fig. 2A-C). Immunostaining against nestin (marker of neural crest stem cells) and SOX10 (key transcription factor expressed in neural crest stem cells) verified the identity of migrated stem cells (Fig. 2D,E) and immunofluorescence staining of cytoskeletal filamentous actin with phalloidin revealed the general morphology of cells (Fig. 2D). Intriguingly, all migrated stem cells were immunofluorescently positive for β III Tubulin and MAP2, which confirm ability of these stem cells to generate neurons in vitro (Fig. 2G,H). A spheroid formation assay revealed that HFSCs can generate tight spheroids in agarose coated plates, providing a three dimensional (3-D) platform for future investigations (Fig. 2I).

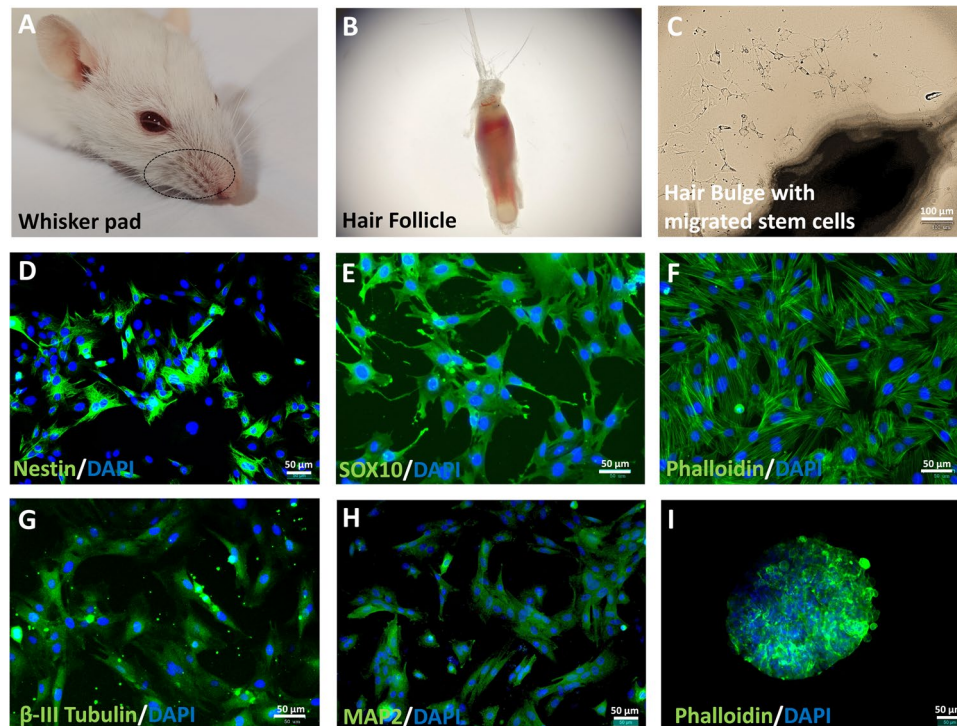


Fig. 2 Hair follicle stem cells in vitro expansion and characteristics. To isolate hair follicle stem cells, the hair follicles of rat whisker pads were dissected (A,B), and the bulge area excised and explanted on collagen coated plates. Few days later, migrated stem cells appeared around the bulges (C), scale bar: 100 μ m. Almost all migrated stem cells are nestin (D) and SOX10 positive (E). Immunostaining of cytoskeletal filamentous actin with phalloidin revealed the general

morphology of migrated stem cells and their cytoskeletal arrangements (F). Also, β III Tubulin (G) and MAP2 (H) expression confirm the ability of these stem cells to generate neurons in vitro. The spheroid formation assay revealed that these stem cells generate tight spheroids in agarose coated plates (I). Cell nuclei were counterstained with DAPI. Images are examples of three different assessments for each immunostaining ($n=3$), scale bar: 50 μ m

Expression of Oxytocin Receptor in Hair Follicle Stem Cells

The assessment of OXTR protein expression in HFSCs by immunostaining revealed that this receptor is expressed abundantly at a level comparable to rat cortical astrocytes and hypothalamic H32 cells. Co-expression of the OXTR and Nestin confirmed the identity of HFSCs (Fig. 3A-D). Here, the expression of OXTR mainly appeared in plasma membrane and cytoplasm. The cytoplasmic and nuclear distribution of the OXTR protein has been observed previously [44, 45]. In fact, G protein-coupled receptors (GPCRs) expression in the cellular membrane can exert cytotoxic effects when it becomes excessive in the expression [46, 47]. Also, culture of these stem cells in presence of FBS that contains oxytocin can lead to OXTR internalization. Therefore, minimal expression of GPCRs at the cell membrane can be expected. In contrast to the protein data, OXTR mRNA levels in HFSCs were significantly lower than in astrocytes (Fig. 3G, H). As evidenced by a cell viability assay, no adverse or cytotoxic effects were detected following 12 h treatment with 100 nM, 500 nM, or 1000 nM OXT (Fig. 3I).

Activation of Downstream Signaling Cascades Following OXT Treatment

We have determined OXTR-coupled intracellular signaling cascades by different doses of OXT (Fig. 4A, B). The MAP kinase ERK1/2 is directly coupled to the OXTR and should be activated first. Indeed, 10 min of OXT stimulation significantly increased the phosphorylation of ERK1/2, with levels returning to baseline thereafter (Fig. 4C). Downstream targets of MAP kinases are transcription factors, such as CREB. In line with the ERK1/2 activation, 100, 500, and 1000 nM OXT also induced phosphorylation of CREB, 10 min following treatment (Fig. 4D). Consequently, any factor that is involved in protein translation has to get activated with a delayed onset, after kinases and transcription factors produced the mRNA. One such factor is eEF2, which has been shown to be activated by OXT via dephosphorylation [39]. In line, we have found decreased phosphorylation of eEF2, 3 h after treatment with 500 or 1000 nM OXT, with continued activation for 12 h with 1000 nM OXT (Fig. 4E).

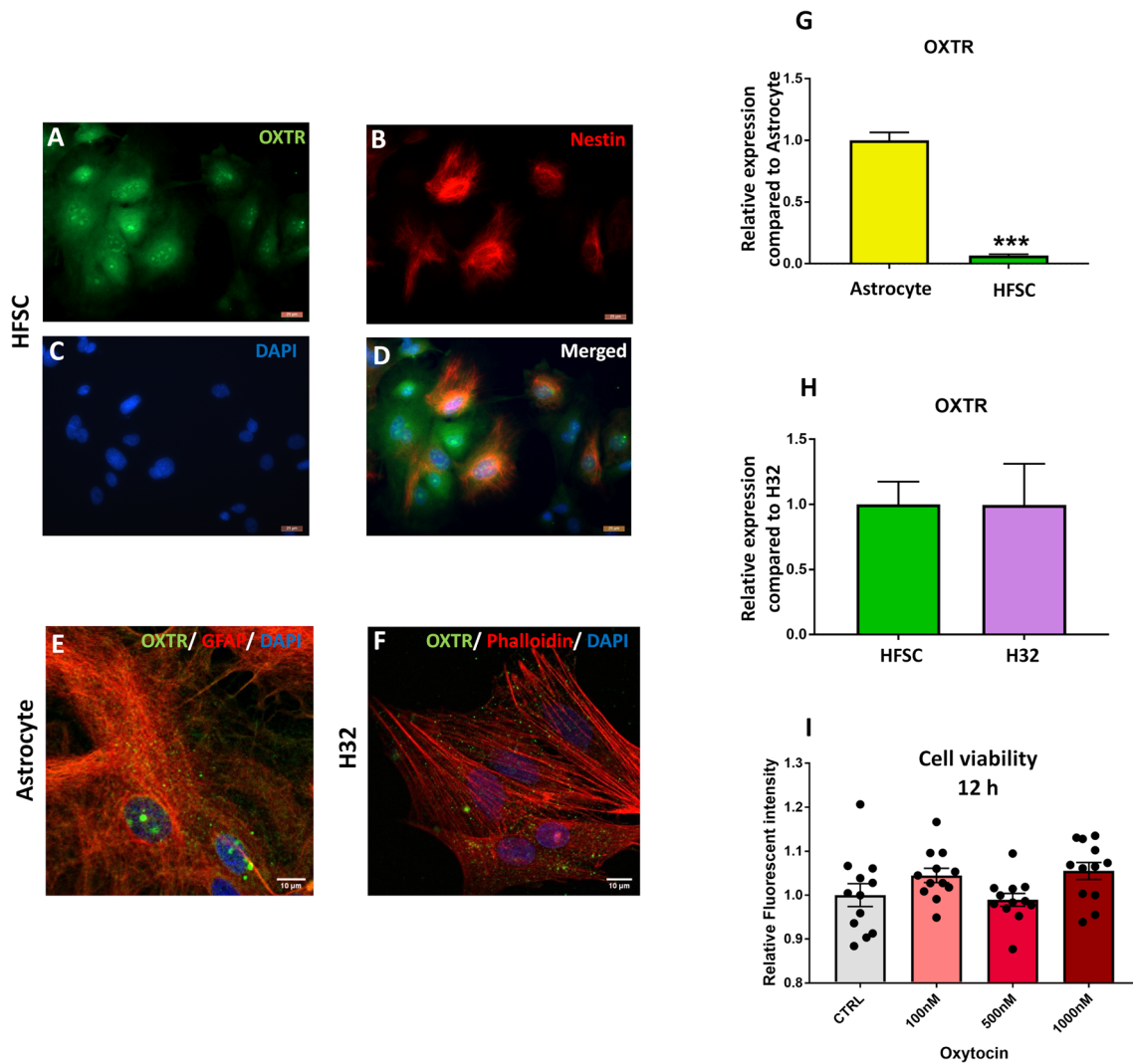


Fig. 3 OXTR expression in hair follicle stem cells. The immunostainings revealed that OXTR expression was co-localized with Nestin expression (A–D), scale bar: 25 μ m. The results confirm that OXTR expression is comparable with cortical astrocytes (E) and H23 cell line (F), scale bar: 25 μ m. Cell nuclei were counterstained

with DAPI. Images are examples of three different assessments for each immunostaining ($n=3$). However, the OXTR gene expression in HFSCs was lower than in astrocytes (G) and almost equal to H32 (H). Also, none of the evaluated concentrations of OXT showed cytotoxic effect on the HFSCs following 12 h treatment (I) ($n=12$)

Effects of OXT on Neurite Outgrowth

Treatment of hair follicle stem cells with 100, 500, or 1000 nM OXT for 10 min, 3 and 12 h significantly elongated the neurites (Fig. 5A–D). As OXT effects can also be mediated via vasopressin receptors, the specificity of OXTR-induced neurite outgrowth was tested using either a specific OXTR agonist (TGOT) or antagonist (L-371,257). Twelve hours of TGOT treatment (100, 500, 1000 nM) resulted in similar effects on neurite length as with OXT, indicating an OXTR-mediated effect only (Fig. 5E). Pre-treatment of hair follicle stem cells with the OXTR antagonist L-371,257 blocked the OXT-induced increase in neurite outgrowth (Fig. 5F).

Effects of OXT on F-Actin Stress Fiber Formation

We made use of the specificity of phalloidin for filamentous actin (F-actin) to unravel cytoskeletal rearrangements induced by synthetic OXT. Due to the effectiveness of the lower OXT doses in the previous experiments we restricted ourselves to 100 and 500 nM of OXT. Treatment of HFSCs with 100 or 500 nM OXT for 10 min significantly increased F-actin accumulation (Fig. 6A). We detected a transient drop in F-actin formation 3 h after the onset of OXT (Fig. 6B), which recovered and even increased above baseline after 12 h of OXT (Fig. 6C). Those actin filaments termed “stress fibers” represent a calcium-dependent

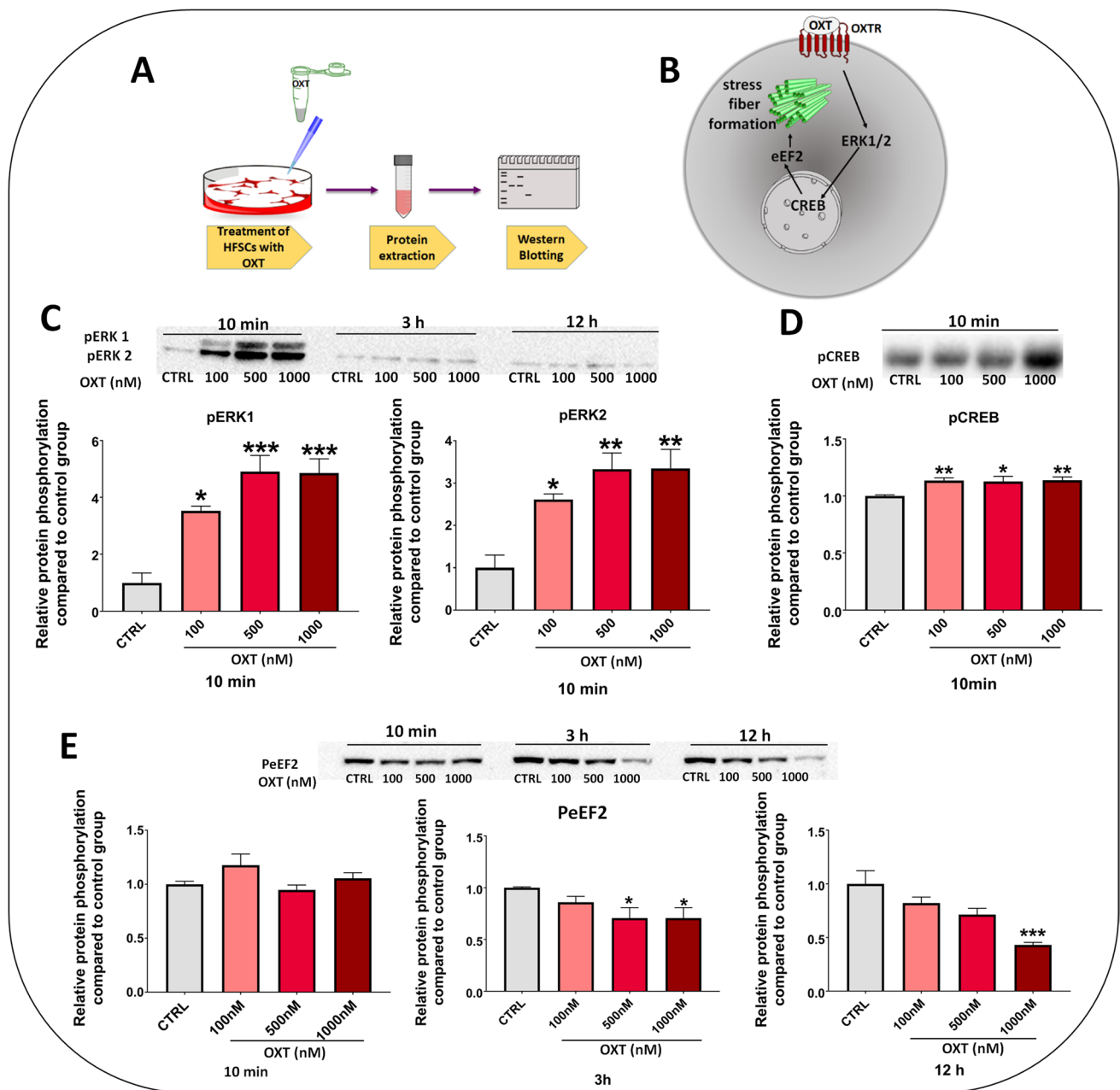


Fig. 4 Activation of selected OXTR-coupled signaling cascades. Schematic representation of the experimental procedure (A). Schematic representation of the OXTR and its coupled signaling cascades (B). Whole cell ERK1/2 phosphorylation is 4–fivefold increased by 100, 500, and 1000 nM of OXT stimulation for 10 min. This increase is transient in nature, as no above-baseline phosphorylation was detected after 3 h or 12 h of OXT stimulation (C). Subse-

quent nuclear activation of CREB by phosphorylation of Ser133 was detected already 10 min after the onset of 100, 500, or 1000 nM of OXT stimulation (D). The elongation factor eEF2 is dephosphorylated, i.e. activated, by 3 h of 500 and 1000 nM of OXT stimulation, and remains to be active for at least 12 h in the 1000 nM OXT treatment group (E). The presented blots are representative of three different immunoblotting ($n=3$)

process that regulates cellular adhesion, migration and morphological alterations [48]. Consequently, OXT treatment could transiently downregulate cytoskeletal rearrangement processes, which return to baseline and even

above baseline after a “chronic” 12-h treatment with OXT. This kind of dichotomy in cellular responses to acute or chronic OXT is in line with our previous findings on behavioral effects of OXT [20, 38, 49, 50].

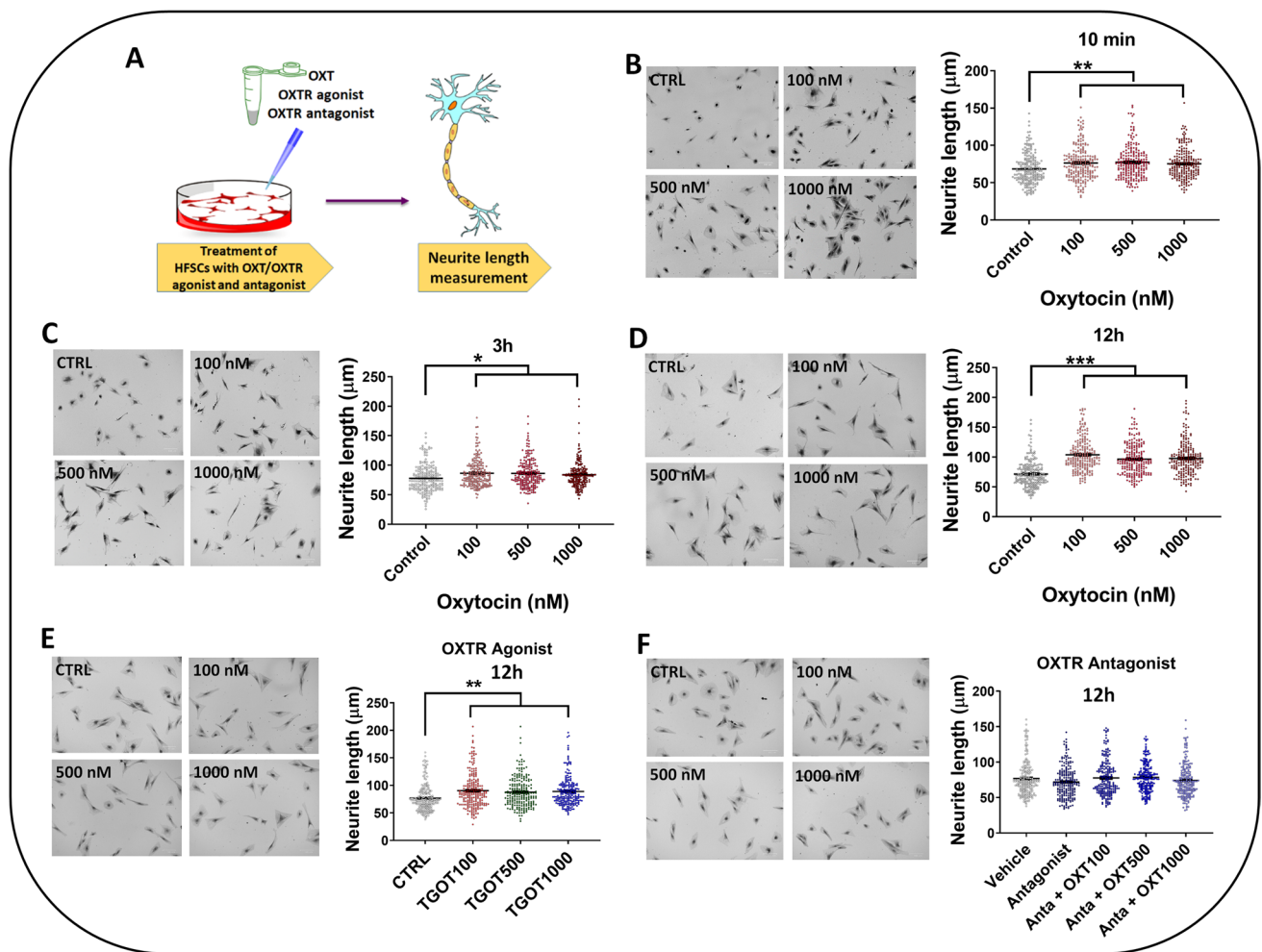


Fig. 5 Neurite outgrowth in response to OXT, OXTR agonist, and OXTR antagonist treatment. Hair follicle stem cells elongate their neurites following treatment with 3 different concentrations of OXT, over the courses of 10 min, 3 h, and 12 h (A, B, C). Also, a 12 h

treatment with the OXTR agonist TGOT resulted in a significant neurite elongation, similar to OXT (D). This OXT-induced effect was blocked by the OXTR antagonist, L-371,257. Scale bar: 100 μm , $n=210$

Discussion

The increasing prevalence of neuropsychiatric disorders highlights the importance of introducing disease-specific models to address the pathophysiology of these disorders and identify novel, targeted treatments. Recent developments in stem cell biology have enabled the culture of patient-derived stem cells that holds enormous potential for unlocking insight into understanding disease mechanisms and drug discovery with higher predictability. In this study, we report the expression of functional OXTR in hair follicle stem cells. Thus, our findings confirm previous reports of OXTR receptor binding sites in the whisker pad follicles of neonatal mice [51] and prairie voles [52], further suggesting a role for the neuropeptide OXT in modulating somatosensory information processing. However, in our study, we detected the expression of OXTR in stem cells

that migrated from the bulge area of rat whisker pad hair follicles. While we obtained strong evidence for specific OXTR expression in the HFSCs, this area is not an exhaustive list of potential areas expressing OXTR. The expression level of OXTR in HFSC migrated from bulge area of rat whisker pad was found to be comparable to rat cortical astrocytes and H32 cells that are known for functional OXTR expression [53, 54]. HFSCs of the bulge region of adult rats are ontologically related to the central nervous system and can differentiate into neurons [55–57] and glial [58–61] cells through minimum manipulation. Therefore, they have been studied for over a decade as a therapeutic option in a variety of animal models of neurological conditions, including spinal cord injury [14, 62, 63], defected sciatic nerve [58, 64, 65], ischemic stroke [16, 17, 66, 67], and vascular dementia [68]. The unique properties of HFSC, such as multipotency and expression of OXTR make them a suitable model system

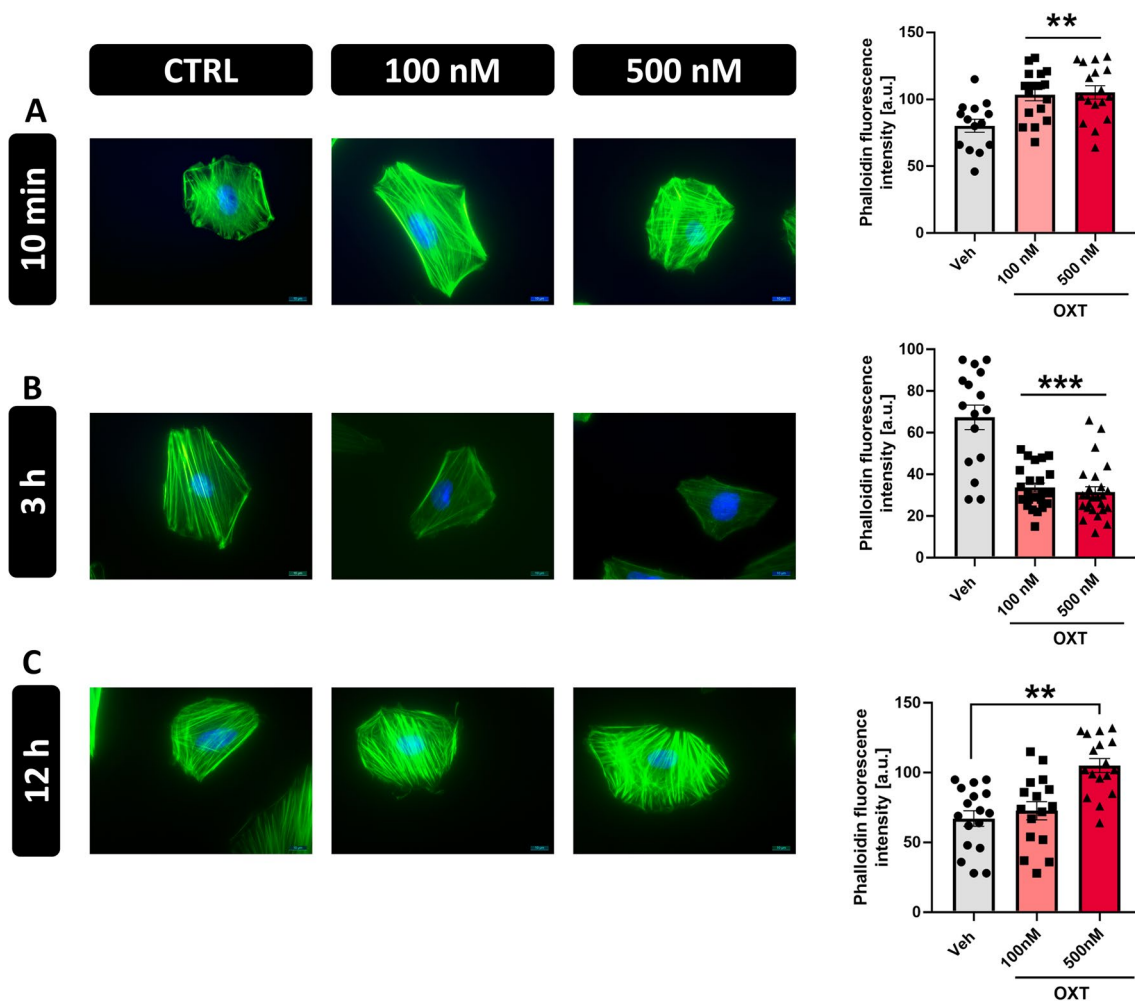


Fig. 6 F-actin dynamic following OXT treatment. Evaluation of cytoskeletal rearrangement induced by OXT revealed that treatment of hair follicle stem cells with 100 and 500 nM OXT for 10 min sig-

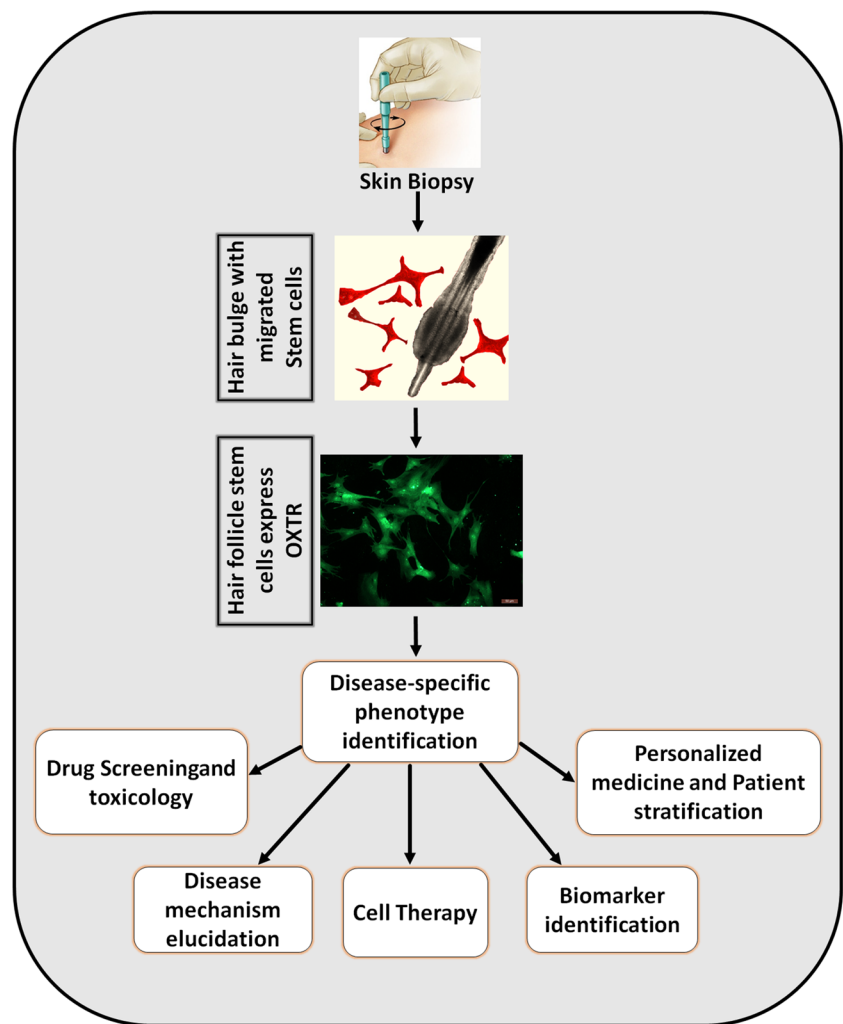
nificantly enhance F-actin accumulation (A). While F-actin formation transiently dropped following 3 h incubation, it returns to base line and over after 12 h treatment. Scale bar: 10 μ m, n = 16

that can recapitulate several aspects of neuropsychiatric disorders in vitro. Thus, the culture of patient-derived stem cells is amenable to large-scale experiments and enables the modeling of individual drug responses. Moreover, once expanded in vitro, genome editing enables the introduction of genetic changes in wild-type stem cells. Intriguingly, these stem cells can form spheroids under appropriate culture conditions which allows a detailed investigation of the neurobiological underpinnings of disease states [69, 70]. It must be noted that albeit OXTR expression was observed in hair follicle stem cells at both mRNA and protein levels, this finding does not provide proof of receptor functionality. To the best of our knowledge, this is the first study that revealed the functionality of OXTR in these stem cells, i.e., the demonstration of activated downstream signaling cascades by OXT treatment. The OXT treatment triggered sequential activation of ERK1/ERK2 and CREB through increasing their phosphorylation, which in turn enhance activation of

eEF2 via reducing its phosphorylation rate. eEF2 is a GTP-binding translation elongation factor. It is an essential factor for protein synthesis. It promotes the GTP-dependent translocation of the nascent protein chain from the A-site to the P-site of the ribosome. The eEF2 dephosphorylation leads to a conformational change that activates eEF2 and leads to increased translation of mRNA into protein.

In addition, OXT treatment stimulated neurite outgrowth in HFSC. In line, Bakos et al. have recently reported the ability of 1 μ M OXT to alter the expression of cytoskeletal proteins associated with growth of neuronal cones, which significantly induced neurite elongation in human SH-SY5Y neuroblastoma cell line [71]. Moreover, OXT affects formation and elongation of the projections in the human U87MG glioblastoma cell line [72]. In 2017, Zatkova and colleagues showed that this effect was mediated by an extracellular calcium influx accompanied by an increase in scaffolding protein SHANK expression [73, 74]. However, Meyer et al.

Fig. 7 Schematic representation of hair follicle stem cells generation and application to use as a patient-derived stem cells model for elucidating disease mechanism, high-throughput drug screening, drug testing and toxicity studies, biomarker identification and patient stratification



provided evidence for the ability of OXT-induced calcium signaling to induce neurite retraction and mitochondrial dysfunction in hypothalamic H32 neural cell line in a dose- and time-dependent manner [75, 76]. These contradicting reports on OXT actions on neurite outgrowth might be explained by cell type-specific effects, or simply by differing OXT concentrations used [47].

Our study also provided evidence for the ability of OXT to induce cytoskeletal rearrangements in HFSC. This morphological alteration is consistent with previous studies that revealed the specific role of ligands of the OXTR in the regulation of gene expression of cytoskeletal proteins in neuroblastoma and glioblastoma cells [77]. Activation of OXTRs enhances the production of inositol-3-phosphate that in turn triggers release of calcium from intracellular stores [78]. This increase of cytosolic calcium and activation of downstream protein kinases lead to cytoskeletal rearrangements [79]. It has been well documented that OXT regulates neuronal morphology, ATP production and calcium signaling [76], which are processes that govern neuronal

connectivity. The neuronal connectivity can be compromised in ASD, which might explain, why some patients benefit from intranasal OXT treatment [80]. Since the remodeling of actin cytoskeleton is considered as one critical factor associated with ASD, several studies investigated whether cytoskeletal dynamics are functionally altered in cells from ASD patients. Recently, Griesi-Oliveira et al. evaluated the regulation of actin cytoskeleton dynamics in stem cells derived from human exfoliated deciduous teeth of ASD patients [81]. They suggested that a significant portion of ASD patients has an abnormal regulation of cytoskeleton dynamics, as revealed in patient-derived stem cells. Consequently, the ability of HFSC to respond to OXT stimulation through activation of downstream signaling pathways, neurite length elongation, and actin cytoskeleton remodeling make them a reliable candidate to model neuropsychiatric disorders with oxytocinergic system deficiency. This hypothesis gains more support from studies that focus on readily obtainable cells from individuals with neuropsychiatric disorders. Considering the limited accessibility of patient brain

biopsies and several challenges of patient derived-iPSCs, increasing attention has thus turned towards olfactory cells [82], exfoliated deciduous teeth, and dental pulp stem cells [83] from living human individuals. These cells offer ex-vivo and in-vitro neuronal cells from individuals, which harbor biological characteristics that probably are more relevant in the context of psychopathologies than skin fibroblasts or blood cells [84]. Since HFSC and the two aforementioned patient-derived cells, share common neural crest origin, we expect the concordance of these stem cells with olfactory and dental stem cells. It is worth noting that we have unpublished data showing high transcript levels of OXTR in human hair follicle stem cells of pubic hair skin biopsies.

Conclusion

Collectively, in this study we demonstrated that hair follicle stem cells isolated from the whisker pad of rats express functional OXTRs. OXTR stimulation by OXT results in activation of intracellular signaling cascades, neurite length alterations, and cytoskeletal rearrangements. Hair follicle stem cells are ontologically related to the nervous system and resemble neurons morphologically and phenotypically. As hair follicle stem cells can be safely obtained from individuals at large scale, they represent a promising model for elucidating disease mechanisms, allow high-throughput drug screening, drug testing and toxicity studies, biomarker identification, and patient stratification in neuropsychiatric disorders associated with OXTR dysregulation (Fig. 7).

Abbreviations ASD: Autism spectrum disorder; GAD: Generalized anxiety disorder; iPSCs: Induced pluripotent stem cells; HFSCs: Hair follicle-derived stem cells; OXTR: Oxytocin receptor; OXT: Oxytocin; SNP: Single nucleotide polymorphisms; eEF2a: Eukaryotic elongation factor 2a

Authors' Contributions SP, MSS and CPM conceptualized the study, performed experiments, analysed the data, and prepared the manuscript draft. BJ, NA and MD involved in manuscript writing, study design, and reviewed and edited the manuscript. IDN substantially reviewed and edited the manuscript and supervised the study and the manuscript.

Funding This study was financially supported by Deutsche Forschungsgemeinschaft (IDN: Ne465/27-1, Ne465/31-1 BJ: JU3039-1), the DFG-GRK 2174 and Iran National Science Foundation (INSF, grant No: 99013300) and Shiraz University of Medical Sciences (Grant No: 27044). Partial support was also provided by International Brain Research Organization (IBRO) Research Fellowship award received by the Mohammad Saied Salehi. The funding body played no role in the design of the study and collection, analysis, and interpretation of data and in writing the manuscript.

Data availability The datasets generated during and/or analyzed during the current study are available from the corresponding author on reasonable request.

Declarations

Ethics Approval and Consent to Participate This project entitled “Evaluation of oxytocin effect on hair follicle-derived stem cells” was approved by the Animal Care Committee of Shiraz University of Medical Sciences, Shiraz, Iran (Approval number: IR.SUMS.AEC.1401.111). All eight rats used in this study were euthanized under CO₂ inhalation in accordance with Guide for the Care and Use of Laboratory Animals by the National Institutes of Health, Bethesda, MD, USA, and approved by the government of the Oberpfalz, Germany. Hair follicles and cortical tissues were immediately obtained from euthanized animals. No experiment was performed on animals. The study is reported in accordance with ARRIVE guidelines.

Consent to Participate Not applicable.

Consent for Publication Not applicable.

Competing Interests The authors declare that they have no competing interests.

References

- Nestler, E. J., & Hyman, S. E. (2010). Animal models of neuropsychiatric disorders. *Nature Neuroscience*, *13*(10), 1161.
- Lago, S. G., Tomasik, J., & Bahn, S. (2021). Functional patient-derived cellular models for neuropsychiatric drug discovery. *Translational Psychiatry*, *11*(1), 1–11.
- Haggarty, S. J., Silva, M. C., Cross, A., Brandon, N. J., & Perlis, R. H. (2016). Advancing drug discovery for neuropsychiatric disorders using patient-specific stem cell models. *Molecular and Cellular Neuroscience*, *73*, 104–115.
- Paşca, S. P., Panagiotakos, G., & Dolmetsch, R. E. (2014). Generating human neurons in vitro and using them to understand neuropsychiatric disease. *Annual Review of Neuroscience*, *37*, 479–501.
- Adegbola, A., Bury, L. A., Fu, C., Zhang, M., & Wynshaw-Boris, A. (2017). Concise review: Induced pluripotent stem cell models for neuropsychiatric diseases. *Stem Cells Translational Medicine*, *6*(12), 2062–2070.
- Haggarty, S. J., & Perlis, R. H. (2014). Translation: Screening for novel therapeutics with disease-relevant cell types derived from human stem cell models. *Biological Psychiatry*, *75*(12), 952–960.
- Wang, M., Zhang, L., & Gage, F. H. (2020). Modeling neuropsychiatric disorders using human induced pluripotent stem cells. *Protein & Cell*, *11*(1), 45–59.
- Hoffman, G. E., Schrode, N., Flaherty, E., & Brennand, K. J. (2019). New considerations for hiPSC-based models of neuropsychiatric disorders. *Molecular Psychiatry*, *24*(1), 49–66.
- Kampmann, M. (2020). CRISPR-based functional genomics for neurological disease. *Nature Reviews Neurology*, *16*(9), 465–480.
- Soliman, M., Aboharb, F., Zeltner, N., & Studer, L. (2017). Pluripotent stem cells in neuropsychiatric disorders. *Molecular Psychiatry*, *22*(9), 1241–1249.
- Vierbuchen, T., Ostermeier, A., Pang, Z. P., Kokubu, Y., Südhof, T. C., & Wernig, M. (2010). Direct conversion of fibroblasts to functional neurons by defined factors. *Nature*, *463*(7284), 1035–1041.
- Yang, N., Ng, Y. H., Pang, Z. P., Südhof, T. C., & Wernig, M. (2011). Induced neuronal cells: How to make and define a neuron. *Cell Stem Cell*, *9*(6), 517–525.
- Pandamooz, S., Naji, M., Alinezhad, F., Zarghami, A., & Pourghasem, M. (2013). The influence of cerebrospinal fluid

- on epidermal neural crest stem cells may pave the path for cell-based therapy. *Stem Cell Research & Therapy*, 4(4), 1–9.
14. Pandamooz, S., Salehi, M. S., Zibaii, M. I., Ahmadiani, A., Nabiuni, M., & Dargahi, L. (2018). Epidermal neural crest stem cell-derived glia enhance neurotrophic elements in an ex vivo model of spinal cord injury. *Journal of Cellular Biochemistry*, 119(4), 3486–3496.
 15. Pandamooz, S., Jafari, A., Salehi, M. S., Jurek, B., Ahmadiani, A., Safari, A., et al. (2020). Substrate stiffness affects the morphology and gene expression of epidermal neural crest stem cells in a short term culture. *Biotechnology and Bioengineering*, 117(2), 305–317.
 16. Salehi, M. S., Pandamooz, S., Safari, A., Jurek, B., Tamadon, A., Namavar, M. R., et al. (2020). Epidermal neural crest stem cell transplantation as a promising therapeutic strategy for ischemic stroke. *CNS Neuroscience & Therapeutics*, 26(7), 670–681.
 17. Karimi-Haghighi, S., Pandamooz, S., Jurek, B., Fattahi, S., Safari, A., Azarpira, N., et al. (2023). From hair to the brain: The short-term therapeutic potential of human hair follicle-derived stem cells and their conditioned medium in a rat model of stroke. *Molecular Neurobiology*, 60, 2587–2601.
 18. Mousavi, S. M., Akbarpour, B., Karimi-Haghighi, S., Pandamooz, S., Belém-Filho, I. J. A., Masis-Calvo, M., et al. (2022). Therapeutic potential of hair follicle-derived stem cell intranasal transplantation in a rat model of ischemic stroke. *BMC Neuroscience*, 23, 47.
 19. Hu, Y. F., Zhang, Z. J., & Sieber-Blum, M. (2006). An epidermal neural crest stem cell (EPI-NCSC) molecular signature. *Stem Cells*, 24(12), 2692–2702.
 20. Jurek, B., & Meyer, M. (2020). Anxiolytic and anxiogenic? how the transcription factor MEF2 might explain the manifold behavioral effects of oxytocin. *Frontiers in Endocrinology*, 11, 186.
 21. Grinevich, V., & Neumann, I. D. (2021). Brain oxytocin: How puzzle stones from animal studies translate into psychiatry. *Molecular Psychiatry*, 26(1), 265–279.
 22. Neumann, I. D., & Landgraf, R. (2012). Balance of brain oxytocin and vasopressin: Implications for anxiety, depression, and social behaviors. *Trends in Neurosciences*, 35(11), 649–659.
 23. Romano, A., Tempesta, B., Micioni Di Bonaventura, M. V., & Gaetani, S. J. F. I. N. (2016). From autism to eating disorders and more: the role of oxytocin in neuropsychiatric disorders. *Frontiers in Neuroscience*, 9, 497.
 24. LoParo, D., & Waldman, I. J. M. P. (2015). The oxytocin receptor gene (OXTR) is associated with autism spectrum disorder: A meta-analysis. *Molecular Psychiatry*, 20(5), 640–646.
 25. Baribeau, D. A., Dupuis, A., Paton, T. A., Scherer, S. W., Schachar, R. J., Arnold, P. D., et al. (2017). Oxytocin receptor polymorphisms are differentially associated with social abilities across neurodevelopmental disorders. *Scientific Reports*, 7(1), 1–11.
 26. Kimura, R., Tomiwa, K., Inoue, R., Suzuki, S., Nakata, M., Awaya, T., et al. (2020). Dysregulation of the oxytocin receptor gene in Williams syndrome. *Psychoneuroendocrinology*, 115, 104631.
 27. Ziegler, C., Dannlowski, U., Bräuer, D., Stevens, S., Laeger, I., Wittmann, H., et al. (2015). Oxytocin receptor gene methylation: Converging multilevel evidence for a role in social anxiety. *Neuropsychopharmacology*, 40(6), 1528–1538.
 28. Uhrig, S., Hirth, N., Broccoli, L., von Wilmsdorff, M., Bauer, M., Sommer, C., et al. (2016). Reduced oxytocin receptor gene expression and binding sites in different brain regions in schizophrenia: A post-mortem study. *Schizophrenia Research*, 177(1–3), 59–66.
 29. Gregory, S. G., Connelly, J. J., Towers, A. J., Johnson, J., Biscocho, D., Markunas, C. A., et al. (2009). Genomic and epigenetic evidence for oxytocin receptor deficiency in autism. *BMC Medicine*, 7(1), 1–13.
 30. Lee, M. R., Sheskier, M., Farokhnia, M., Feng, N., Marenco, S., Lipska, B., et al. (2018). Oxytocin receptor mRNA expression in dorsolateral prefrontal cortex in major psychiatric disorders: A human post-mortem study. *Psychoneuroendocrinology*, 96, 143–147.
 31. King, L. B., Walum, H., Inoue, K., Eyrich, N. W., & Young, L. J. J. B. P. (2016). Variation in the oxytocin receptor gene predicts brain region-specific expression and social attachment. *Biological Psychiatry*, 80(2), 160–169.
 32. Danoff, J. S., Wroblewski, K. L., Graves, A. J., Quinn, G. C., Perkeybile, A. M., Kenkel, W. M., et al. (2021). Genetic, epigenetic, and environmental factors controlling oxytocin receptor gene expression. *Clinical Epigenetics*, 13(1), 1–16.
 33. Takayanagi, Y., Yoshida, M., Bielsky, I. F., Ross, H. E., Kawamata, M., Onaka, T., et al. (2005). Pervasive social deficits, but normal parturition, in oxytocin receptor-deficient mice. *Proceedings of the National Academy of Sciences of the United States of America*, 102(44), 16096–16101.
 34. Wei, J., Ma, L., Ju, P., Yang, B., Wang, Y.-X., & Chen, J. (2020). Involvement of oxytocin receptor/Erk/MAPK signaling in the mPFC in early life stress-induced autistic-like behaviors. *Frontiers in Cell and Developmental Biology*, 8, 564485.
 35. Horiai, M., Otsuka, A., Hidema, S., Hiraoka, Y., Hayashi, R., Miyazaki, S., et al. (2020). Targeting oxytocin receptor (Oxtr)-expressing neurons in the lateral septum to restore social novelty in autism spectrum disorder mouse models. *Scientific Reports*, 10(1), 1–13.
 36. Tomizawa, K., Iga, N., Lu, Y.-F., Moriwaki, A., Matsushita, M., Li, S.-T., et al. (2003). Oxytocin improves long-lasting spatial memory during motherhood through MAP kinase cascade. *Nature Neuroscience*, 6(4), 384–390.
 37. Jurek, B., Slattery, D. A., Maloumy, R., Hiller, K., Koszinowski, S., Neumann, I. D., et al. (2012). Differential contribution of hypothalamic MAPK activity to anxiety-like behaviour in virgin and lactating rats. *PLoS ONE*, 7(5), e37060.
 38. Jurek, B., Slattery, D. A., Hiraoka, Y., Liu, Y., Nishimori, K., Aguilera, G., et al. (2015). Oxytocin regulates stress-induced Crf gene transcription through CREB-regulated transcription coactivator 3. *Journal of Neuroscience*, 35(35), 12248–12260.
 39. Martinecz, S., Meinung, C.-P., Jurek, B., von Schack, D., van den Burg, E. H., Slattery, D. A., et al. (2019). De novo protein synthesis mediated by the eukaryotic elongation factor 2 is required for the anxiolytic effect of oxytocin. *Biological Psychiatry*, 85(10), 802–811.
 40. Flavell, S. W., Cowan, C. W., Kim, T.-K., Greer, P. L., Lin, Y., Paradis, S., et al. (2006). Activity-dependent regulation of MEF2 transcription factors suppresses excitatory synapse number. *Science*, 311(5763), 1008–1012.
 41. Schildge, S., Bohrer, C., Beck, K., Schachtrup, C. (2013). Isolation and culture of mouse cortical astrocytes. *Journal of visualized experiments*, 71, 50079.
 42. Pandamooz, S., Jurek, B., Dianatpour, M., Haerteis, S., Limm, K., Oefner, P. J., et al. (2023). The beneficial effects of chick embryo extract preconditioning on hair follicle stem cells: A promising strategy to generate Schwann cells. *Cell Proliferation*, 56(7), e13397.
 43. Bustin, S. A., Benes, V., Garson, J. A., Hellemans, J., Huggett, J., Kubista, M., et al. (2009). The MIQE guidelines: Minimum information for publication of quantitative real-time PCR experiments. *Clinical Chemistry*, 55(4), 611–622.
 44. Di Benedetto, A., Sun, L., Zamboni, C. G., Tamma, R., Nico, B., Calvano, C. D., et al. (2014). Osteoblast regulation via ligand-activated nuclear trafficking of the oxytocin receptor. *Proceedings of the National Academy of Sciences*, 111(46), 16502–16507.
 45. Conti, F., Sertic, S., Reversi, A., & Chini, B. (2009). Intracellular trafficking of the human oxytocin receptor: Evidence of

- receptor recycling via a Rab4/Rab5 “short cycle.” *American Journal of Physiology-Endocrinology and Metabolism*, 296(3), E532–E542.
46. Meyer, M., Jurek, B., Alfonso-Prieto, M., Ribeiro, R., Milenkovic, V. M., Winter, J., et al. (2022). Structure-function relationships of the disease-linked A218T oxytocin receptor variant. *Molecular Psychiatry*, 27(2), 907–917.
 47. Jurek, B., & Neumann, I. D. (2018). The oxytocin receptor: From intracellular signaling to behavior. *Physiological Reviews*, 98(3), 1805–1908.
 48. Tojkander, S., Ciuba, K., & Lappalainen, P. (2018). CaMKK2 regulates mechanosensitive assembly of contractile actin stress fibers. *Cell Reports*, 24(1), 11–19.
 49. Winter, J., & Jurek, B. (2019). The interplay between oxytocin and the CRF system: Regulation of the stress response. *Cell and Tissue Research*, 375(1), 85–91.
 50. Winter, J., Meyer, M., Berger, I., Royer, M., Bianchi, M., Kuffner, K., et al. (2021). Chronic oxytocin-driven alternative splicing of Crfr2 α induces anxiety. *Molecular Psychiatry*. <https://doi.org/10.1038/s41380-021-01141-x>
 51. Greenwood, M. A., & Hammock, E. A. (2017). Oxytocin receptor binding sites in the periphery of the neonatal mouse. *PLoS ONE*, 12(2), e0172904.
 52. Greenwood, M. A., & Hammock, E. A. (2019). Oxytocin receptor binding sites in the periphery of the neonatal prairie vole. *Frontiers in Neuroscience*, 13, 474.
 53. Wahis, J., Baudon, A., Althammer, F., Kerspern, D., Goyon, S., Hagiwara, D., et al. (2021). Astrocytes mediate the effect of oxytocin in the central amygdala on neuronal activity and affective states in rodents. *Nature Neuroscience*, 24(4), 529–541.
 54. Van Den Burg, E. H., Stindl, J., Grund, T., Neumann, I. D., & Strauss, O. (2015). Oxytocin stimulates extracellular Ca²⁺ influx through TRPV2 channels in hypothalamic neurons to exert its anxiolytic effects. *Neuropsychopharmacology*, 40(13), 2938–2947.
 55. Amoh, Y., Li, L., Katsuoaka, K., Penman, S., & Hoffman, R. M. (2005). Multipotent nestin-positive, keratin-negative hair-follicle bulge stem cells can form neurons. *Proceedings of the National Academy of Sciences of the United States of America*, 102(15), 5530–5534.
 56. Narytnyk, A., Verdon, B., Loughney, A., Sweeney, M., Clewes, O., Taggart, M. J., et al. (2014). Differentiation of human epidermal neural crest stem cells (hEPI-NCSC) into virtually homogeneous populations of dopaminergic neurons. *Stem Cell Reviews and Reports*, 10(2), 316–326.
 57. Yamane, M., Takaoka, N., Obara, K., Shirai, K., Aki, R., Hamada, Y., et al. (2021). Hair-follicle-associated pluripotent (HAP) stem cells can extensively differentiate to tyrosine-hydroxylase-expressing dopamine-secreting neurons. *Cells*, 10(4), 864.
 58. Lin, H., Liu, F., Zhang, C., Zhang, Z., Guo, J., Ren, C., et al. (2009). Pluripotent hair follicle neural crest stem-cell-derived neurons and schwann cells functionally repair sciatic nerves in rats. *Molecular Neurobiology*, 40(3), 216–223.
 59. Sakaue, M., & Sieber-Blum, M. (2015). Human epidermal neural crest stem cells as a source of Schwann cells. *Development*, 142(18), 3188–3197.
 60. Pournajaf, S., Valian, N., Shalmani, L. M., Khodabakhsh, P., Jorjani, M., & Dargahi, L. (2020). Fingolimod increases oligodendrocytes markers expression in epidermal neural crest stem cells. *European Journal of Pharmacology*, 885, 173502.
 61. Khodabakhsh, P., Pournajaf, S., Mohaghegh Shalmani, L., Ahmadiani, A., & Dargahi, L. (2021). Insulin promotes Schwann-like cell differentiation of rat epidermal neural crest stem cells. *Molecular Neurobiology*, 58(10), 5327–5337.
 62. Hu, Y. F., Gourab, K., Wells, C., Clewes, O., Schmit, B. D., & Sieber-Blum, M. (2010). Epidermal neural crest stem cell (EPI-NCSC)—mediated recovery of sensory function in a mouse model of spinal cord injury. *Stem Cell Reviews and Reports*, 6(2), 186–198.
 63. Obara, K., Shirai, K., Hamada, Y., Arakawa, N., Yamane, M., Takaoka, N., et al. (2022). Chronic spinal cord injury functionally repaired by direct implantation of encapsulated hair-follicle-associated pluripotent (HAP) stem cells in a mouse model: Potential for clinical regenerative medicine. *PLoS ONE*, 17(1), e0262755.
 64. Li, Y., Yao, D., Zhang, J., Liu, B., Zhang, L., Feng, H., et al. (2017). The effects of epidermal neural crest stem cells on local inflammation microenvironment in the defected sciatic nerve of rats. *Frontiers in Molecular Neuroscience*, 10, 133.
 65. Zhang, L., Li, B., Liu, B., & Dong, Z. (2019). Co-transplantation of epidermal neural crest stem cells and olfactory ensheathing cells repairs sciatic nerve defects in rats. *Frontiers in Cellular Neuroscience*, 13, 253.
 66. Mousavi, S. M., Akbarpour, B., Karimi-Haghighi, S., Pandamooz, S., Belém-Filho, I. J. A., Masis-Calvo, M., et al. (2022). Therapeutic potential of hair follicle-derived stem cell intranasal transplantation in a rat model of ischemic stroke. *BMC Neuroscience*, 23(1), 1–14.
 67. Zhang, X., Tang, H., Mao, S., Li, B., Zhou, Y., Yue, H., et al. (2020). Transplanted hair follicle stem cells migrate to the penumbra and express neural markers in a rat model of cerebral ischaemia/reperfusion. *Stem Cell Research & Therapy*, 11(1), 1–12.
 68. Akbari, S., Hooshmandi, E., Bayat, M., Haghighi, A. B., Salehi, M. S., Pandamooz, S., et al. (2022). The neuroprotective properties and therapeutic potential of epidermal neural crest stem cells transplantation in a rat model of vascular dementia. *Brain Research*, 1776, 147750.
 69. Quadrato, G., Brown, J., & Arlotta, P. (2016). The promises and challenges of human brain organoids as models of neuropsychiatric disease. *Nature Medicine*, 22(11), 1220–1228.
 70. Salehi, M. S., Neumann, I. D., Jurek, B., & Pandamooz, S. (2021). Co-stimulation of oxytocin and arginine-vasopressin receptors affect hypothalamic neurospheroid size. *International Journal of Molecular Sciences*, 22(16), 8464.
 71. Lestanova, Z., Bacova, Z., Kiss, A., Havranek, T., Strbak, V., & Bakos, J. (2016). Oxytocin increases neurite length and expression of cytoskeletal proteins associated with neuronal growth. *Journal of Molecular Neuroscience*, 59(2), 184–192.
 72. Lestanova, Z., Puerta, F., Alanazi, M., Bacova, Z., Kiss, A., Castejon, A., et al. (2017). Downregulation of oxytocin receptor decreases the length of projections stimulated by retinoic acid in the U-87MG cells. *Neurochemical Research*, 42(4), 1006–1014.
 73. Zatkova, M., Reichova, A., Bacova, Z., Strbak, V., Kiss, A., & Bakos, J. (2018). Neurite outgrowth stimulated by oxytocin is modulated by inhibition of the calcium voltage-gated channels. *Cellular and Molecular Neurobiology*, 38(1), 371–378.
 74. Zatkova, M., Bacova, Z., Puerta, F., Lestanova, Z., Alanazi, M., Kiss, A., et al. (2018). Projection length stimulated by oxytocin is modulated by the inhibition of calcium signaling in U-87MG cells. *Journal of Neural Transmission*, 125(12), 1847–1856.
 75. Meyer, M., Berger, I., Winter, J., & Jurek, B. (2018). Oxytocin alters the morphology of hypothalamic neurons via the transcription factor myocyte enhancer factor 2A (MEF-2A). *Molecular and Cellular Endocrinology*, 477, 156–162.
 76. Meyer, M., Kuffner, K., Winter, J., Neumann, I. D., Wetzel, C. H., & Jurek, B. (2020). Myocyte enhancer factor 2A (MEF2A) defines oxytocin-induced morphological effects and regulates mitochondrial function in neurons. *International Journal of Molecular Sciences*, 21(6), 2200.
 77. Bakos, J., Strbak, V., Paulikova, H., Krajnakova, L., Lestanova, Z., & Bacova, Z. (2013). Oxytocin receptor ligands induce changes in cytoskeleton in neuroblastoma cells. *Journal of Molecular Neuroscience*, 50(3), 462–468.

78. Gimpl, G., & Fahrenholz, F. (2001). The oxytocin receptor system: Structure, function, and regulation. *Physiological Reviews*, 81(2), 629–683.
79. Wang, Y.-F., & Hatton, G. I. (2007). Interaction of extracellular signal-regulated protein kinase 1/2 with actin cytoskeleton in supraoptic oxytocin neurons and astrocytes: Role in burst firing. *Journal of Neuroscience*, 27(50), 13822–13834.
80. Parker, K. J., Oztan, O., Libove, R. A., Sumiyoshi, R. D., Jackson, L. P., Karhson, D. S., et al. (2017). Intranasal oxytocin treatment for social deficits and biomarkers of response in children with autism. *Proceedings of the National Academy of Sciences of the United States of America*, 114(30), 8119–8124.
81. Griesi-Oliveira, K., Suzuki, A. M., Alves, A. Y., Mafra, A. C. C. N., Yamamoto, G. L., Ezquina, S., et al. (2018). Actin cytoskeleton dynamics in stem cells from autistic individuals. *Scientific Reports*, 8(1), 1–10.
82. Unterholzner, J., Millischer, V., Wotawa, C., Sawa, A., & Lanzemberger, R. (2021). Making sense of patient-derived iPSCs, trans-differentiated neurons, olfactory neuronal cells, and cerebral organoids as models for psychiatric disorders. *International Journal of Neuropsychopharmacology*, 24(10), 759–775.
83. Masuda, K., Han, X., Kato, H., Sato, H., Zhang, Y., Sun, X., et al. (2021). Dental pulp-derived mesenchymal stem cells for modeling genetic disorders. *International Journal of Molecular Sciences*, 22(5), 2269.
84. Borgmann-Winter, K., Willard, S., Sinclair, D., Mirza, N., Turetsky, B., Berretta, S., et al. (2015). Translational potential of olfactory mucosa for the study of neuropsychiatric illness. *Translational Psychiatry*, 5(3), e527–e527.

Publisher's Note Springer Nature remains neutral with regard to jurisdictional claims in published maps and institutional affiliations.

Springer Nature or its licensor (e.g. a society or other partner) holds exclusive rights to this article under a publishing agreement with the author(s) or other rightsholder(s); author self-archiving of the accepted manuscript version of this article is solely governed by the terms of such publishing agreement and applicable law.

Terms and Conditions

Springer Nature journal content, brought to you courtesy of Springer Nature Customer Service Center GmbH (“Springer Nature”).

Springer Nature supports a reasonable amount of sharing of research papers by authors, subscribers and authorised users (“Users”), for small-scale personal, non-commercial use provided that all copyright, trade and service marks and other proprietary notices are maintained. By accessing, sharing, receiving or otherwise using the Springer Nature journal content you agree to these terms of use (“Terms”). For these purposes, Springer Nature considers academic use (by researchers and students) to be non-commercial.

These Terms are supplementary and will apply in addition to any applicable website terms and conditions, a relevant site licence or a personal subscription. These Terms will prevail over any conflict or ambiguity with regards to the relevant terms, a site licence or a personal subscription (to the extent of the conflict or ambiguity only). For Creative Commons-licensed articles, the terms of the Creative Commons license used will apply.

We collect and use personal data to provide access to the Springer Nature journal content. We may also use these personal data internally within ResearchGate and Springer Nature and as agreed share it, in an anonymised way, for purposes of tracking, analysis and reporting. We will not otherwise disclose your personal data outside the ResearchGate or the Springer Nature group of companies unless we have your permission as detailed in the Privacy Policy.

While Users may use the Springer Nature journal content for small scale, personal non-commercial use, it is important to note that Users may not:

1. use such content for the purpose of providing other users with access on a regular or large scale basis or as a means to circumvent access control;
2. use such content where to do so would be considered a criminal or statutory offence in any jurisdiction, or gives rise to civil liability, or is otherwise unlawful;
3. falsely or misleadingly imply or suggest endorsement, approval, sponsorship, or association unless explicitly agreed to by Springer Nature in writing;
4. use bots or other automated methods to access the content or redirect messages
5. override any security feature or exclusionary protocol; or
6. share the content in order to create substitute for Springer Nature products or services or a systematic database of Springer Nature journal content.

In line with the restriction against commercial use, Springer Nature does not permit the creation of a product or service that creates revenue, royalties, rent or income from our content or its inclusion as part of a paid for service or for other commercial gain. Springer Nature journal content cannot be used for inter-library loans and librarians may not upload Springer Nature journal content on a large scale into their, or any other, institutional repository.

These terms of use are reviewed regularly and may be amended at any time. Springer Nature is not obligated to publish any information or content on this website and may remove it or features or functionality at our sole discretion, at any time with or without notice. Springer Nature may revoke this licence to you at any time and remove access to any copies of the Springer Nature journal content which have been saved.

To the fullest extent permitted by law, Springer Nature makes no warranties, representations or guarantees to Users, either express or implied with respect to the Springer nature journal content and all parties disclaim and waive any implied warranties or warranties imposed by law, including merchantability or fitness for any particular purpose.

Please note that these rights do not automatically extend to content, data or other material published by Springer Nature that may be licensed from third parties.

If you would like to use or distribute our Springer Nature journal content to a wider audience or on a regular basis or in any other manner not expressly permitted by these Terms, please contact Springer Nature at

onlineservice@springernature.com